Materials Plus
https://ojs.wiserpub.com/index.php/MP/

Research Article

Bayesian Uncertainty Update to a Model of Flexural Strength of α-SiC

Eric A. Walker*, Jason Sun, James Chen*

Department of Mechanical and Aerospace Engineering, University at Buffalo- The State University of New York Jarvis Hall, Mary Putnam Way Amherst, NY 14260, USA
E-mail: ericwalk@buffalo.edu; chenjm@buffalo.edu

Received: 1 February 2024; **Revised:** 6 March 2024; **Accepted:** 8 March 2024

Abstract: This article demonstrates a statistical method to update the uncertainty in the flexural strength of silicon carbide, α-SiC. The previously reported uncertainty for the flexural strength of α-SiC was a constant ±15%. However, this uncertainty should be adjusted as more data becomes available. A Bayesian approach is proposed to rapidly and precisely update the uncertainty. To validate the method, five scenarios are demonstrated. The first scenario assumes the experimental data is distributed as the model predicts. The second and third scenarios have the model underestimating and overestimating flexural strength, respectively. The fourth and fifth scenarios use data from a thermo-mechanical fracture model. The thermo-mechanical fracture model introduces a change in the temperature transition of flexural strength. The uncertainty decreased from 15% to a range between 8.3% and 13.4%. Two parameters are inferred in the fourth scenario while five are inferred in the fifth scenario. Inferring five parameters leads to more consistent uncertainty across temperature.

Nomenclature

α	A parameter in the flexural strength model
β	A parameter in the flexural strength model
γ	A parameter in the flexural strength model that controls the steepness of the temperature transition
δ	A parameter in the flexural strength model that controls the midpoint of the temperature transition
ε	Model inadequacy
ζ	A parameter in the flexural strength model
θ	The set of parameters α, β, γ, δ, ε, ζ
θ'	The proposal set of parameters in the random walk algorithm
δ_ε	Standard deviation of the model inadequacy. The model inadequacy accounts for uncertainty due to the model itself and uncertainty due to the experimental error
δ_Q	Standard deviation of the step size in the random walk algorithm
$p(\theta)$	Prior probability density function (PDF) of the parameter set
$p(FS^*\|\theta)$	Likelihood of the observed flexural strength data given the parameter values
$p(FS^*)$	Model evidence, a normalizing factor
$p(\theta\|FS^*)$	Posterior PDF of parameters
FS	Flexural strength (MPa)
Q	Step taken in the random walk algorithm
T	Temperature ℃

DOI: https://doi.org/10.37256/3120244395

1. Introduction

In the field of Integrated Computational Materials Engineering (ICME), uncertainty in model predictions is unavoidable [1]. There are multiple sources of uncertainty in ICME and a thorough uncertainty quantification (UQ) is challenging. A recent publication reported a UQ of an experimental data set of α-SiC [2]. However, Štubňa, et al. [2] focus on the uncertainty of a fixed set of data and does not allow for real-time update. What is needed for the ceramics manufacturing community is a live uncertainty update as new data becomes available [3]. The flexural strength of α-SiC specimens vary due to inconsistencies in manufacturing processes [4]. For example, machining tools undergo wear and form imperfections leading to microstructure and surface defects [5−7]. These wears are major sources of uncertainty in the flexural strength of α-SiC. A wide variety of manufacturing techniques, from ultrasonically vibrating the workpiece [8] to water jets [9], aim at alleviating the surface defects but do not entirely remove them [10]. These unavoidable defects cause inconsistency in ceramic product performance. An uncertainty update from the most recent testing data will support the consistent quality of ceramics in production.

Ceramic Matrix Composites (CMC's) have the advantage of being resistant to high temperatures and light weight. The temperature limit before weakening of CMC's with a SiC matrix (the part that is not fiber) is ~1800 ℃. Some interesting applications of CMC's are brake discs for cars, high-speed trains and elevators [11]. They are candidate materials for nuclear fuel cladding [12] and hypersonic aeroengines [13]. At smaller size, they are a promising as a semiconductor material [14]. Gas turbines are yet another application of CMC's [15]. These produce electricity from a fuel gas, such as natural gas or hydrogen. Yet again, the high temperature resilience and low density are cited as advantages of CMC's. In this article, the flexural strength of α-SiC and its uncertainty are modeled over a range of temperatures, 0 ℃ to 1600 ℃. A Bayesian uncertainty update demonstrates how different synthetic data sets influence the uncertainty [16]. In addition, the number of inferred model parameters is discussed. One may envision this tool as a quality assurance tool for manufacturing or a comparison tool for testing manufacturing methods.

There exists a need for methods that update uncertainty in a model as new data becomes available. Such methods have been developed and implemented with varying levels of maturity [17]. An example of updating model predictions and uncertainty are the state of charge and state of health of a battery [18]. One of the oldest yet of proven practical importance, for example in guidance and navigation, is the Kalman filter [19]. This method makes assumptions about model linearity and all uncertainties being of a Gaussian distribution. The extended Kalman filter removes some of the nonlinearity by obtaining an approximate Jacobian [20]. The unscented Kalman filter expands to a general non-linear model but retains Gaussian distributions [21]. A particle filter does use Bayes' formula [18], but obtaining the particles is done more cheaply than the Markov chains of batch Bayesian inference. In the application here, destructive bending tests of ceramic bars provide updated data much slower than the time needed for a batch Bayesian inference. The method applied in this article is most accurately classified as batch Bayesian inference.

The term *credible intervals* is used when describing the uncertainty distributions [22]. *Credible interval* makes a distinction from the frequentist view of probability. The uncertainty here derives from a lack of knowledge of the flexural strength of the SiC bar, though it was in fact determined by its manufacturing process. If one knew the exact process parameters by which a ceramic was produced along with a perfectly accurate physical model, the flexural strength of the bar would be known exactly.

There have been a number of studies using Bayesian methods for ceramics. Oh et al. [23] used a sporadic data set of 82 data points with which to find important chemical properties or features, in predicting the critical thin film thickness to achieve stress relaxation. The machine-learning models they compared were nearest-neighbor regression, kernel ridge regression, Bayesian ridge regression and a support vector machine. The feature sets of material properties were organized qualitatively into four sets, including ionic properties, general phase features and others. The Bayesian ridge regression was shown to be the most consistently accurate in predicting critical thickness for stress relaxation. Portune et al. [24] used a Bayesian update on a UQ of the transition velocity of ceramic armor material. The transition velocity is the minimum velocity for a projectile to penetrate a material. These works suggested the effectiveness of the Bayesian approach. However, Bayesian statistics have not yet been explicitly applied to flexural strength, which is one of the important ceramics performance indicators.

In industry, when new material suppliers are included or new sub-contracts are retained,} the quality of the final product constantly needs to be re-evaluated. The proposed Bayesian statistics tool can be used to investigate various scenarios and manage the uncertainty caused by the new change [25]. In this study, a Bayesian approach is used to investigate the impact of the change on the uncertainty. The prior model is consistent in all scenarios from the experimental data from literature [26]. The prior data is from the leading Munro uncertainty quantification model. Though problematic, it is the best starting point from which to perform tests and evaluate

various scenarios. Munro's ±15% absolute bounds [26] translated to the 95% credible interval here. The scenarios are a broad view of plausible changes in flexural strength over temperature due to a new change in a manufacturing environment. The scenarios cannot be comprehensive, though, because there are infinite possible flexural strength changes that could be encountered. However, the model evidence is an indicator when the model begins to fail and cannot reconcile with the experimental data. Taken in another way, model evidence is a tool to assess that the model is still reliable and that the Bayesian update from the experimental data is operating properly.

Here, the Theory/Calculation section lays out the Bayesian update framework in the context of flexural strength of α-SiC as a function of temperature. The Bayesian update algorithm is summarized. The Results and Discussion section states the specifics of the scenarios and computational decisions related to the random walk algorithm that implements the Bayesian update. The improvements in goodness-of-fit and uncertainty bounds for each of the scenarios is reported. The first three scenarios make use of synthetic experimental data with one inferred parameter. The fourth and fifth scenarios use thermo-mechanical fracture model data [27]. The difference between the fourth scenario and the fifth scenario is the number of inferred parameters. The fourth scenario infers two, and the fifth scenario infers all five of the model parameters. Comparison of the model evidence between the fourth and fifth scenarios illustrates how to choose the number of inferred parameters. The overall result is a useful and general tool to manage uncertainty in α-SiC other than universally using ±15%. All code to reproduce this work is available [28].

2. Theory and calculation

Each instance that Bayesian inference is applied to a new model and new data sets, there arise questions about how to set the likelihood hyperparameter and which parameters to infer. In addition, in the case of the model and data in this article, there multiple data points from a temperature interval, making a data set that is treated as a single multidimensional data point. The likelihood accounts for each deviation from a model prediction and the result of a bend test at each temperature. Subsequent to the Bayesian inference, three metrics evaluate the posterior results. First, the change in the 95% credible interval is computed and reported. The goal is to reduce this credible interval from prior to posterior. Second, the R^2 of the mean of the credible interval to the data measures the goodness-of-it. Still, the credible interval is a distribution that contains more information than the mean. Therefore, the Kullback-Leibler divergence measures the change in the distribution [29, 30]. No change would be a Kullback-Leibler divergence of zero. While the model in this article contains five parameters, a test is made for whether inferring only two parameters is more effective. The Bayesian concept of model evidence [30] is used to formally make that determination here. Using the same data set, the model evidences from inferring two parameters and five parameters are compared.

The flexural strength model from Munro [26] is,

$$FS(MPa) = \left(359 + \frac{87.6}{1 + 208600e^{-0.012T}}\right) \pm 15\% \tag{1}$$

FS is flexural strength (MPa) and T (°C) is temperature with an uncertainty of ±15%. The values in Equation 1 are replaced with parameters to yield,

$$FS(MPa) = \left(\alpha + \frac{\beta}{1 + e^{-\gamma(T-\delta)}}\right)\zeta + \epsilon \tag{2}$$

$\alpha, \beta, \gamma, \delta$ and ζ are parameters. γ controls the steepness of the slope of the flexural strength transition and δ controls the temperature center point of this transition. ϵ is the model inadequacy to predict experiments beyond the parameter uncertainty.

The original uncertainty of ±15% is a uniform probability density function (PDF). In contrast, parameters in this article are modeled with a Gaussian. In a Gaussian PDF, 68%, 95% and 99.5% of the data fall within one, two and three standard deviations of the mean, respectively.

Bayes' formula is,

$$p(\theta|FS^*) = \frac{p(FS^*|\theta)p(\theta)}{p(FS^*)} \tag{3}$$

In Equation 3, the *prior* uncertainty, $p(\theta)$, is model uncertainty before an experimental observation data set arrives [31]. The *posterior* uncertainty, $p(\theta|FS^*)$, is the result of the Bayesian update [32]. The *likelihood*, $p(FS^*|\theta)$, is a PDF returning the probability of a prediction and its distance to experimental observations. The *model evidence*, $p(FS^*)$, is a normalizing term. The model evidence ensures the integral of the posterior PDF equals one.

For the prior in this article, a Gaussian PDF of Equation 4 with a reasonable shape is assigned to each parameter. The likelihood is also Gaussian, i.e.,

$$p(FS^*|\theta) = \frac{1}{\sqrt{2\pi}\sigma_\epsilon} e^{-\frac{\sum_T (FS_T - FS_T^*)^2}{\sigma_\epsilon^2}} \quad (4)$$

θ is the set of parameters containing $\alpha, \beta, \gamma, \delta \; and \; \zeta$. Experimental data for flexural strength is denoted FS_T^*. When the experimental observation is further away from the model prediction, FS_T, the likelihood $p(FS^*|\theta)$ decreases. The asterisk, *, denotes benchmark data which is either synthetic data or predictions from a thermos-mechanical fracture model. The T index is for the various temperatures at which there are flexural strength transitions. For any given θ, there are multiple flexural strength predictions and data over the temperature range. Therefore, a summation is taken over temperature, T, in the likelihood.

Equation 4 has introduced a hyperparameter, σ_ϵ. A hyperparameter is a parameter that is not in original model, but it appears in Bayes' formula. By necessity, a Gaussian PDF must have this standard deviation, σ_ϵ. The choice of value for σ_ϵ influences the result of Bayes' formula. Fortunately, there are clear indications when a poor choice of σ_ϵ has been made. A poor σ_ϵ will lead to the reduction of model evidence or an increase in uncertainty. Between these two extremes, a smaller σ_ϵ drives the posterior more to goodness-of-fit to the data and away from the prior. An interpretation of σ_ϵ is the standard deviation of model inadequacy. A model is inadequate because it is often a simplified representation and does not account for measurement error. Although *model inadequacy* refers strictly to the model and not the measurement error [22], in this article the terms are lumped together in model inadequacy.

A random walk algorithm is used to sample the posterior, $p(\theta|FS^*)$. A numerical approach is needed because the data is a non-linear function over temperature and data across temperature are used in the Bayesian inference [31]. The model contains exponents that are by nature highly non-linear. The exponent is also in the denominator with two terms. An analytical solution would be effective for a polynomial model but not for this model. By design, the random walk algorithm samples proportionally to the probability. The samples therefore form the PDF. Metropolis-Hastings Markov Chain Monte Carlo (MCMC) is used in this study [31]. The MCMC takes proposal sample around the current sample. A proposal sample, θ' is taken as shown by Equation 5.

$$\theta' = \theta + Q \quad (5)$$

In this article, Q is randomly sampled from an identical Gaussian PDF as the prior, $p(\theta)$. The covariance of Q is a diagonal matrix with the diagonal entries based upon the prior variance of the parameters. Q does not have to be exactly the prior, but it is a justified choice because it ensures that the proposal samples are on the same scale as the parameters. The exact accept or reject probability of any proposal step is [31],

$$p(\theta') = \begin{cases} 1, & when \; \frac{p(FS*|\theta')p(\theta')}{p(FS*|\theta)p(\theta)} \geq 1 \\ \frac{p(FS*|\theta')p(\theta')}{p(FS*|\theta)p(\theta)}, & when \; \frac{p(FS*|\theta')p(\theta')}{p(FS*|\theta)p(\theta)} < 1 \end{cases} \quad (6)$$

The mean of the prior is chosen as the starting point of the MCMC in this article. The beginning of the MCMC samples are cut out as part of the burn-in process when computing the posterior PDF. The burn-in samples are needed because the posterior distribution is not known before the MCMC starts. Both the number of burn-in samples and the total number of samples are selected to accurately generate a consistent posterior.

Kullback-Leibler divergence is computed to measure the amount of learning for each parameter that is inferred. Kullback-Leibler divergence is defined in Equation 7.

$$D_K L(P||Q) = \int_x p(x) log_2 \left(\frac{p(x)}{q(x)}\right) \quad (7)$$

$D_K L(P||Q)$ is the Kullback-Leibler divergence of PDF P from PDF Q. PDF P is the posterior and PDF Q is the prior. x is the parameter that is being evaluated. For example, x is ζ in scenarios 1-3. When divide-by-zero of log-of-zero is encountered, the integration area contributes zero.

In the first scenario, it is assumed that the mean from the prior data sets stay unchanged. The prior data sets [26] are a collection of four experimental data sources [33–36]. In one of those sources, the α-SiC was doped with ZrO_2 [33]. Another source was of $SiC - TiB_2$ composites [34]. Therefore, the prior data sets are a less than perfect representation of α-SiC, since they contain a variety of SiC. Nonetheless, the purpose of this scenario is to demonstrate that the uncertainty shrinks as data confirms the model predictions. The prior was set to replicate the $\pm 15\%$ credible interval from literature as much as possible. The experimental data that led to the $\pm 15\%$ credible interval from Munro [26] is not used a second time at all in the scenarios in the current work. Rather, synthetic experimental data is created and also data from a high-fidelity thermo-mechanical fracture model is used [27]. Beyond taken the literature precedent for prior uncertainty, reasonable prior uncertainties are assigned to parameters such that the prior model prediction is not completely uncertain yet uncertain enough to allow for adapting to new data. The second and third scenarios have noisy data with an added and subtracted mean of 25 (MPa), respectively. The second scenario is the case of the model underestimating the flexural strength, and the

third scenario is the model overestimating the flexural strength. The fourth scenario uses multiple data representing different material properties at each temperature as predicted by a thermo-mechanical fracture model implemented in the MOOSE software framework [27]. The fourth scenario exhibits a late temperature transition in flexural strength and a second parameter is inferred. The fifth scenario uses the same data but uses all five parameters for inference. The Bayesian model evidence is used to compare the fourth and fifth scenarios to weight goodness-of-fit versus overfitting (Occam's razor) in choosing the best course. The data in the first three scenarios is independent and identically distributed. In the fourth and fifth scenarios, the data are from physics model prediction.

3. Results and discussion

The uncertainty decreases in all of the five scenarios, and the goodness-of-fit based upon the mean improves. The number of samples is 250,000, and the burn-in number of samples is 10,000. In the first scenario, synthetic experimental data is generated by adding zero-mean noise to the model. The standard deviation of the noise is set to 20 (MPa). In the likelihood, σ_ϵ is likewise set to 20 (MPa). It should be noted that knowing the amount of ordinary variation is helpful in selecting σ_ϵ for different applications. The posterior uncertainty of scenario one was 11.2% at lower temperatures (20 ℃ to 600 ℃) and 9.1% at higher temperatures, compared to the prior 15% uncertainty. This uncertainty numbers are the 99.5% credible interval.

In the second scenario, an underestimation of flexural strength may be due to increasing residence time during chemical vapor infiltration (CVI) [15]. Alternatively, a proper temperature and pressure regime for a CVI precursor may achieve almost no excess Si [37]. These steps may increase flexural strength (the second scenario). An overall overestimation of flexural strength in the third scenario may be due to a more defective manufacturing than thought previously. For instance, a finishing tool could be worn and chipped [38]. The second and third scenarios use a shift of 25 (MPa) from the prior model mean. The choice of 20 (MPa) for σ_ϵ matches the added noise and leads to reasonable prior and likelihood probabilities. Scenario two results in 10.2% uncertainty at low temperatures (20 ℃ to 600 ℃) and 8.2% uncertainty at higher temperatures. Scenario three's posterior uncertainty is 11.6% at low temperatures (20 ℃ to 600 ℃) and 9.4% at high temperatures. These results are summarized in Table 1. The credible interval is defined as 99.5% of the probability. The 99.5% is the same as three standard deviations above or below the mean. The results of the underestimation and overestimation scenarios are displayed in Figure 1.

At this juncture, data from a thermo-mechanical fracture model is introduced for scenarios four and five [27, 39]. Thus far, the first three scenarios have involved synthetic experimental data inferring one parameter, ζ. Inferring these two parameters, δ and ζ, from the thermo-mechanical fracture model data is scenario four. The thermo-mechanical fracture model data exhibits a late-temperature transition in flexural strength. Inferring δ allows for changing the midpoint of a temperature transition to match. It is known that SiC forms oxidation layers at high temperatures [11]. Such oxidation layers are the physical source of the temperature transition in flexural strength [26]. The oxidizing conditions and the material itself influence the formation of oxide layers. Consequently, oxide layers cause a noticeable change in flexural strength as a function of temperature. However, the temperature effect is not consistently observed. Ghosh et al. [36] found no change in flexural strength over their tested temperature range of 0–1400 ℃. Becher [35] detected a slight upward transition at a lower temperature starting at less than 1000 ℃. Therefore, the model should be able to adapt to data with a different flexural strength transition over temperature. The fourth scenario does change the temperature transition, as seen in Figure 2, and as evidenced by an increase in R^2 from zero to 0.57. The posterior uncertainty is 11.6% at low temperatures (20 ℃ to 600 ℃) and 13.4% at high temperatures.

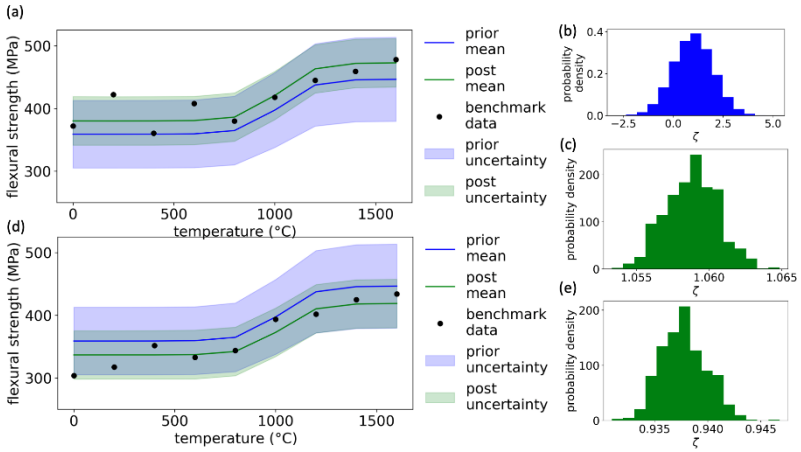

Figure 1. Bayesian update for scenarios two and three. (a) Synthetic data shifted up (scenario two). (b) ζ parameter prior (c) ζ parameter posterior scenario two. (d) Synthetic data shifted down (scenario three). (e) ζ parameter posterior scenario three

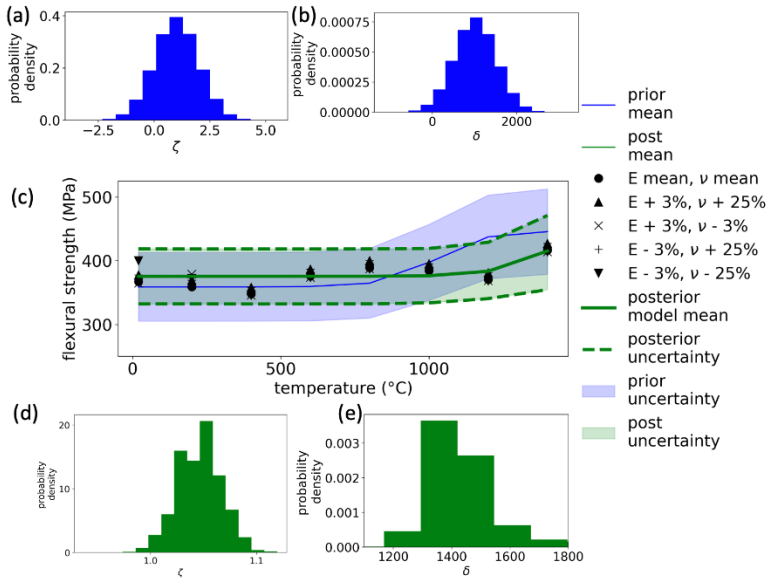

Figure 2. Thermo-mechanical fracture model data in the fourth scenario. Two parameters are inferred. (a) ζ parameter prior. (b) δ parameter prior. (c) Prior and posterior flexural strength with uncertainty from Bayesian update. (d) ζ parameter posterior. (e) δ parameter posterior. δ parameter has shifted right from its prior of 1020

Table 1. Improvement in credible intervals and learning as measured by Kullback-Leibler divergence

	Low temperature uncertainty	High temperature uncertainty	Kullback-Leibler divergence
Scenario 1- centered	11.2%	9.1%	1.28
Scenario 2- shifted up	10.2%	8.2%	1.33
Scenario 3- shifted down	11.6%	9.4%	1.31
Scenario 4- Thermo-mechanical fracture model	11.6%	13.4%	$\delta = 6.8 \times 10^{-4}$ $\zeta = 0.90$
Scenario 5- Thermo-mechanical fracture model with five parameters	11.6%	12.1%	$\delta = 8.8 \times 10^{-4}$ $\zeta = 0.79$

The fifth scenario serves the purpose of testing model evidence. The fifth scenario uses the data from the thermo-mechanical fracture model, the same data as the fourth scenario. The model evidence for using all five parameters was 2×10^{-8} while the model evidence for inferring two parameters was 9×10^{-6}. Nonetheless, the uncertainty level is more consistent across temperature than the fourth scenario, i.e., the uncertainty is between 11.6% and 12.1%. As more data becomes available, the uncertainty will decrease, unless the data is conflicting. This is the most consistent uncertainty across temperature for all of the scenarios. The difference from the fourth scenario is that all of the parameters are updated with Bayesian statistics. With more relaxed parameters, the model is more free to fit to the data.

The consistent uncertainty across temperature suggests that the overall shape of the data has been captured better than the fourth scenario. The model evidence is three orders of magnitude less. The decrease in model evidence is from the extra parameters causing shrinking prior probabilities. In principal, inferring more parameters allows for a better goodness-of-fit when the experimental data curve is very different from the prior model curve. It should be noted that inferring more model parameters is built-in penalty in Bayesian statistics for over-fitting the data. This is useful to know because it is a mistake to over-fit to the data.

The parameters in this article have been modeled with Gaussian distributions. However, ceramic failures may be defined by Weibull PDF's. As a test, the ζ parameter that controls the uncertainty bounds can be set to a Weibull PDF prior. Using scenario three as an example, the resulting posterior from the Bayesian update yields an uncertainty bound of $\pm 11.5\%$ at low temperatures (20 ℃ to 600 ℃) and $\pm 9.3\%$ at high temperatures. The Weibull prior provides only a marginal improvement to the Gaussian prior.

σ_ϵ may be inferred as a hyperparameter to yield the best results. When inferring σ_ϵ in Scenario 4, the maximum uncertainty at low temperatures is 11.4% and 13.6% at high temperatures. The results in terms of reducing uncertainty are an improvement because the uncertainty was reduced at every temperature except at the single highest temperature point. The mean σ_ϵ was inferred to be 24.5 (MPa) compared to the estimated 20 (MPa).

The results reported in this article are batch Bayesian inferences. It is conceivable in a manufacturing environment that Bayesian inferences would be conducted online. In that way, the posterior becomes the prior until the next set of data arrives. This is referred to as a particle filter [18]. In addition, the Bayesian paradigm is capable to expand to more complex multi-scale models [40].

4. Conclusions

This work has placed uncertainty management in a rigorous mathematical framework (exact, flexible, scalable and rapid). Previously, uncertainty quantification was only performed with heuristics and statistics for one batch of data without the ability of a real-time update with regards to ceramics' flexural strength. The Bayesian update reconciles prior uncertainties with new data that arrives. The variations of the test scenarios in this article rigorously validate the flexibility of this approach. The uncertainty has decreased from a constant 15% to between 8.2% and 13.4%. However, every model is different, and an expert choice on the standard deviation of model inadequacy is necessary. Fortunately, model evidence provides feedback on this choice. The model evidence for using all five parameters was 2×10^{-8} while the model evidence for inferring two parameters was 9×10^{-6}. When the likelihood numbers drop to being minuscule, the model evidence decreases as well. The Bayesian approach has been shown to be effective in the context of bending tests to obtain flexural strength of a range of temperatures for α-SiC ceramic. One future direction is to develop a surrogate model like the one used here, but mixed with with physically meaningful parameters, such as Young's modulus.

Acknowledgments

Funding for this project was provided, in part, by LIFT, the Detroit-based national manufacturing innovation institute operated by ALMMII, the American Lightweight Materials Manufacturing Innovation Institute, a Michigan-based nonprofit, 501(c)3 as part of ONR Grant N00014-21-1-2660. The authors are grateful to Dr. Amberlee Haselhuhn and Dr. David Hicks for the constructive discussions.

References

[1] Panchal, J. H., Kalidindi, S. R., and McDowell, D. L., 2013, “Key computational modeling issues in integrated computational materials engineering,” Computer-Aided Design, 45, pp. 4–25.

[2] ˇStubˇna, I., Sˇ´ın, P., Trn´ık, A., and Voz´ar, L., 2019, “Measuring the flexural strength of ceramics at elevated temperatures – an uncertainty analysis,” Measurement Science Review, 14, pp. 1195–1203.

[3] Fertig, A., Weigold, M., and Chen, Y., 2022, “Ma-chine learning based quality prediction for milling processes using internal machine tool data,” Advances in Industrial and Manufacturing Engineering, 4, p. 100074.

[4] Dong, G., Lang, C., Li, C., and Zhang, L., 2020, "Formation mechanism and modelling of exit edge-chipping during ultrasonic vibration grinding of deep-small holes of microcrystalline-mica ceramics," Ceramics International, 46, pp. 12458–12469.
[5] Yin, T., To, S., Du, H., and Zhang, G., 2022, "Effects of wheel spindle error motion on surface generation in grinding," International Journal of Mechanical Sciences, 218, p. 107046.
[6] Meng, B., Yuan, D., and Xu, S., 2019, "Study on strain rate and heat effect on the removal mechanism of sic during nano-scratching process by molecular dynamics simulation," International Journal of Mechanical Sciences, 151, pp. 724–732.
[7] Fung, K., Tang, C., and Cheung, C., 2017, "Molecular dynamics analysis of the effect of surface flaws of diamond tools on tool wear in nanometric cutting," Computational Materials Science, 133, pp. 60–70.
[8] Yan, L., Zhang, X., Li, H., and Zhang, Q., 2022, "Machinability improvement in three-dimensional (3d) ultrasonic vibration assisted diamond wire sawing of sic," Ceramics International, 48, pp. 8051–8068.
[9] Wang, J., 2007, "Predictive depth of jet penetration models for abrasive waterjet cutting of alumina ceramics," International Journal of Mechanical Sciences, 49, pp. 306–316.
[10] Liu, J., Ye, C., and Dong, Y., 2021, "Recent development of thermally assisted surface hardening techniques: A review," Advances in Industrial and Manufacturing Engineering, 2, p. 100006.
[11] Arai, Y., Inoue, R., Goto, K., and Kogo, Y., 2019, "Carbon fiber reinforced ultra-high temperature ceramic matrix composites: A review," Ceramics International, 45, pp. 14481–14489.
[12] Nagaraju, H. T., Nance, J., Kim, N. H., Sankar, B., and Subhash, G., 2023, "Uncertainty quantification in elastic constants of sicf/sicm tubular composites using global sensitivity analysis," Journal of Composite Materials, 57(1), pp. 63–78.
[13] An, Q., Chen, J., Ming, W., and Chen, M., 2021, "Machining of sic ceramic matrix composites: A review," Chinese Journal of Aeronautics, 34(4), pp. 540–567.
[14] Kashyap, A., Chen, C.-P., Ghandi, R., Patil, A., Andarawis, E., Yin, L., Shaddock, D., Sandvik, P., Fang, K., Shen, Z., and Johnson, R., 2013, "Silicon carbide integrated circuits for extreme environments," pp. 60–63.
[15] Cha, C. M., Liliedahl, D., Sankaran, R., and Ramanuj, V., 2022, "Microstructural and infiltration properties of woven preforms during chemical vapor infiltration," Journal of the American Ceramic Society, 105, p. 4595–4607.
[16] Mahadevan, S., Nath, P., and Hu, Z., 2022, "Un-certainty Quantification for Additive Manufacturing Process Improvement: Recent Advances," ASCE-ASME J Risk and Uncert in Engrg Sys Part B Mech Engrg, 8.
[17] S¨arkk¨a, S., 2013, Bayesian Filtering and Smoothing Institute of Mathematical Statistics Textbooks. Cambridge University Press.
[18] Walker, E., Rayman, S., and White, R. E., 2015, "Comparison of a particle filter and other state estimation methods for prognostics of lithium-ion batteries," Journal of Power Sources, 287, pp. 1–12.
[19] Kalman, R. E., 1960, "A New Approach to Linear Filtering and Prediction Problems," Journal of Basic Engineering, 82(1), pp. 35–45.
[20] Terejanu, G. A., et al. "Extended Kalman filter tutorial,".
[21] Terejanu, G. A. "Unscented Kalman filter tutorial,".
[22] Kennedy, M. C., and O'Hagan, A., 2001, "Bayesian calibration of computer models," Journal of the Royal Statistical Society: Series B (Statistical Methodology), 63(3), pp. 425–464.
[23] Oh, J. Y., Shin, D., and Choi, W. S., 2023, "Ap-plication of machine learning to sporadic experimental data for understanding epitaxial strain relaxation," Journal of the American Ceramic Society, 106, pp. 780–788.
[24] Portune, A. R., and Hilton, C. D., 2013, "Determination of uncertainty in transition velocity estimates for ceramic materials," International Journal of Ap-plied Ceramic Technology, 10, pp. 107–113.
[25] Tuncel, G., and Alpan, G., 2010, "Risk assessment and management for supply chain networks: A case study," Computers in Industry, 61, pp. 250–259.
[26] Munro, R. G., 1997, "Material properties of a sintered alpha-sic," Journal of Physical and Chemical Reference Data, 26, pp. 1195–1203.
[27] Sun, J., Chen, Y., Marziale, J. J., Walker, E. A., Salac, D., and Chen, J., 2022, "Damage prediction of sintered alpha-sic using thermo-mechanical coupled fracture model," Submitted.
[28] https://github.com/ChenReaction/managing_uncertainty, March, 2024.
[29] Walker, E., Ammal, S. C., Terejanu, G. A., and Hey-den, A., 2016, "Uncertainty quantification framework applied to the water–gas shift reaction over pt-based catalysts," The Journal of Physical Chemistry C, 120(19), pp. 10328–10339.

[30] Walker, E. A., Mitchell, D., Terejanu, G. A., and Heyden, A., 2018, "Identifying active sites of the water–gas shift reaction over titania supported platinum catalysts under uncertainty," ACS Catalysis, 8(5), pp. 3990–3998.
[31] Walker, E. A., Ravisankar, K., and Savara, A., 2020, "Chekipeuq intro 2: Harnessing uncertainties from data sets, bayesian design of experiments in chemical kinetics**," ChemCatChem, 12, pp. 5401–5410.
[32] Kuhn, J., Spitz, J., Sonnweber-Ribic, P., Schneider, M., and B¨ohlke, T., 2021, "Identifying material parameters in crystal plasticity by bayesian optimization," Optimization and Engineering, 23, pp. 1489–1523.
[33] Hecht, N. L., Goodrich, S. M., McCullum, D. E., Yaney, P. P., Jang, S. D., and Tennery, V. J., 1992, "Characterization studies of transformation-toughened ceramics," Ceramic Bulletin, 71.
[34] McMurtry, C. H., Boecker, W. D. G., Seshadri, S. G., Zanghi, J. S., and Garnier, J. E., 1987, "Microstructure and material properties of sic-tib2 particulate composites," American Ceramic Society Bulletin, 66.
[35] Becher, P. F., 1984, "Strength degradation in sic and si3n4 ceramics by exposure to coal slags at high temperatures," Journal of Materials Science, 19, pp. 2805–2814.
[36] Ghosh, A., Jenkins, M. G., White, K. W., Kobayashi, A. S., and Bradt, R. C., 1989, "Elevated-temperature fracture resistance of a sintered α-silicon carbide," Journal of the American Ceramic Society, 72, pp. 242–247.
[37] Desenfant, A., Laduye, G., Vignoles, G. L., and Chollon, G., 2021, "Kinetic and gas-phase study of the chemical vapor deposition of silicon carbide from c2h3sicl3/h2," Journal of Industrial and Engineering Chemistry, 94, pp. 145–158.
[38] Wang, J., Chi, H., Lv, M., Liu, X., Li, Y., and Zhao, Y., 2020, "Effect of silicon carbide hard particles scratch on the diamond cutting tools groove wear," Proceedings of the Institution of Mechanical Engineers, Part C: Journal of Mechanical Engineering Science, 234, pp. 2053–2063.
[39] Sun, J., Marziale, J. J., Haselhuhn, A. S., Salac, D., and Chen, J., 2024, "An ICME framework for short fiber reinforced ceramic matrix composites via direct ink writing," Modelling and Simulation in Materials Science and Engineering, 32(2), p. 025007.
[40] Kimaev, G., Chaffart, D., and Ricardez-Sandoval, L. A., 2020, "Multilevel Monte Carlo applied for uncertainty quantification in stochastic multiscale systems," AIChE Journal, 66, p. e16262.